

Article

Factors Controlling the Spatial and Temporal Variability in Groundwater ^{222}Rn and U Levels

Soo Young Cho ¹, Min-Ho Koo ², Byong Wook Cho ¹, Youn-Young Jung ³ and Yong Hwa Oh ^{1,*}

¹ Groundwater Research Center, Geologic Environment Division, Korea Institute of Geoscience and Mineral Resources, Daejeon 34142, Korea

² Department of Geoenvironmental Sciences, Kongju National University, Kongju 32588, Korea

³ Division of Earth and Environmental Sciences, Korea Basic Science Institute, Chungbuk 24341, Korea

* Correspondence: yonghwa.oh@gmail.com

Received: 26 July 2019; Accepted: 28 August 2019; Published: 29 August 2019



Abstract: Radon (^{222}Rn) and uranium (U) measurements were conducted in 98 groundwater samples in Yongin area, Korea to identify the factors controlling their levels and spatial distributions. Groundwater samples were obtained from the different depth of wells used for drinking water and irrigation. ^{222}Rn and U concentrations were measured using a liquid scintillation counter (LSC) equipped with a pulse-shape analyzer and inductively coupled plasma mass spectrometers (ICP-MS), respectively. Large variations were observed in groundwater concentrations of ^{222}Rn and U, ranging between 0.6 ± 0.1 – 673.7 ± 8.7 Bq L⁻¹ and 0.02–117.00 µg L⁻¹, respectively. Correlation analysis revealed no significant relationship between field parameters (temperature, electrical conductivity, pH, and dissolved oxygen) and ^{222}Rn or U concentrations. The fact that ^{222}Rn and U concentrations were higher in granite areas than gneiss areas suggests that lithology plays a significant role in controlling the levels and spatial distributions of the two radionuclides. Furthermore, groundwater ^{222}Rn and U behaviors have been affected by the existence of fault and well depth. Especially, the temporal monitoring of ^{222}Rn suggests that ^{222}Rn concentrations in the shallow groundwater may be controlled by variation in rainfall and artificial effects such as water curtain cultivation conducted in the winter season in this study area.

Keywords: radon; uranium; groundwater; geological characteristics; correlation analysis

1. Introduction

Groundwater has been a globally essential resource for drinking, industrial, and agricultural purposes throughout history. For example, over 95% of the rural population depends on groundwater for their drinking water in the USA [1]. In Korea, groundwater provides 13% (approximately 3.7 billion m³) of the total annual water supply, and the use of groundwater is increasing continuously [2]. Human consumption of groundwater, however, may be restricted due to quality concerns. Naturally occurring radionuclides in groundwater, such as radon (^{222}Rn) and uranium (U), have become major health issues with previous studies reporting high radionuclide levels [3–5].

^{222}Rn is a naturally occurring radionuclide with a half-life of 3.8 days. Due to its suitable half-life and high concentration in groundwater, ^{222}Rn has been used as an excellent tracer for quantifying groundwater discharge and determining groundwater-surface water interaction in aquatic systems such as streams, rivers, wetlands, and estuaries [6–10]. Furthermore, ^{222}Rn in groundwater has been monitored worldwide to predict earthquakes and understand natural processes [11–13]. U, a redox sensitive element, has been used to examine the portion of submarine groundwater discharge in coastal zones because its concentration and isotopic ratio ($^{234}\text{U}/^{238}\text{U}$) presented different endmembers in seawater and coastal groundwater [14,15]. Although there are various applications of ^{222}Rn and U

in the scientific researches, the excess dissolved radionuclides (^{222}Rn and U) in groundwater used for drinking water can impact the human health. Inhaling or ingesting ^{222}Rn is known to cause lung and stomach cancer [16,17]. U can cause kidney problems, and its inhalation presents a chemical toxicity risk to the lungs [18,19].

Previous studies have reported on the spatial distributions and levels of ^{222}Rn and U in groundwater and drinking water in other countries. For example, ^{222}Rn and U concentrations were measured in 5097 wells located in more than 40 principals in USA, showing that 2.7% of the groundwater samples contained ^{222}Rn concentrations which were higher than the alternative maximum contaminant level (AMCL) of 148 Bq L^{-1} recommended by US EPA (Environmental Protection Agency) [20]. In India, ^{222}Rn and ^{238}U groundwater concentrations from 41 different locations were reported to range from 0.86 to 7.62 Bq L^{-1} and from 0.26 to $29 \mu\text{g L}^{-1}$, respectively, indicating that high levels of these radionuclides were associated with lithology [3]. In Korea, recently, ^{222}Rn concentrations in 3818 groundwater samples were measured and 26.5% of the total samples exceeded the World Health Organization (WHO) radon level limit of 100 Bq L^{-1} [21]. It is reported that approximately 4% of 4140 wells in South Korea contained U concentrations exceeding the WHO guideline level for drinking water, $30 \mu\text{g L}^{-1}$ [22], suggesting that these groundwater wells should be closed immediately to reduce health hazards [23].

With this background, the need to determine ^{222}Rn and U distributions and concentrations in groundwater is significant, especially in regions where residents use groundwater containing high ^{222}Rn and U levels for drinking. Therefore, this study was conducted in Yongin area where high ^{222}Rn concentrations have already been reported [24] and groundwater has been used for drinking water and irrigation. This study aimed (1) to investigate the levels and spatial distributions of ^{222}Rn and U in groundwater and (2) to determine the factors controlling these radionuclides' behaviors in Yongin area, Korea.

2. Materials and Methods

2.1. Site Description

Groundwater samples were collected from wells in Yongin area (185 km^2) located in the northwest part of South Korea (Figure 1). The mean annual precipitation and temperature of this region are 1560 mm and $11 \text{ }^\circ\text{C}$, respectively, with high precipitation concentrated in the summer monsoon season (June and July). The basement rock primarily consists of Jurassic gneissose biotite granite (over 70% of the study area) and Precambrian banded gneiss [24,25]. Jurassic gneissose biotite granite is composed of biotite and hornblende, and Precambrian banded gneiss is composed of quartz, plagioclase, and biotite [25].

2.2. Groundwater Sampling

Groundwater samples were collected from 98 groundwater wells located in Yongin area in 2013. Samples were taken after the wells were purged by pumping for more than 15 min using a submersible pump to remove well bore storage. Field parameters including temperature, electrical conductivity (EC), pH, and dissolved oxygen (DO) in groundwater were measured in situ using portable meters (Orion 5 Star). Well depths varied from 25 to 200 m.

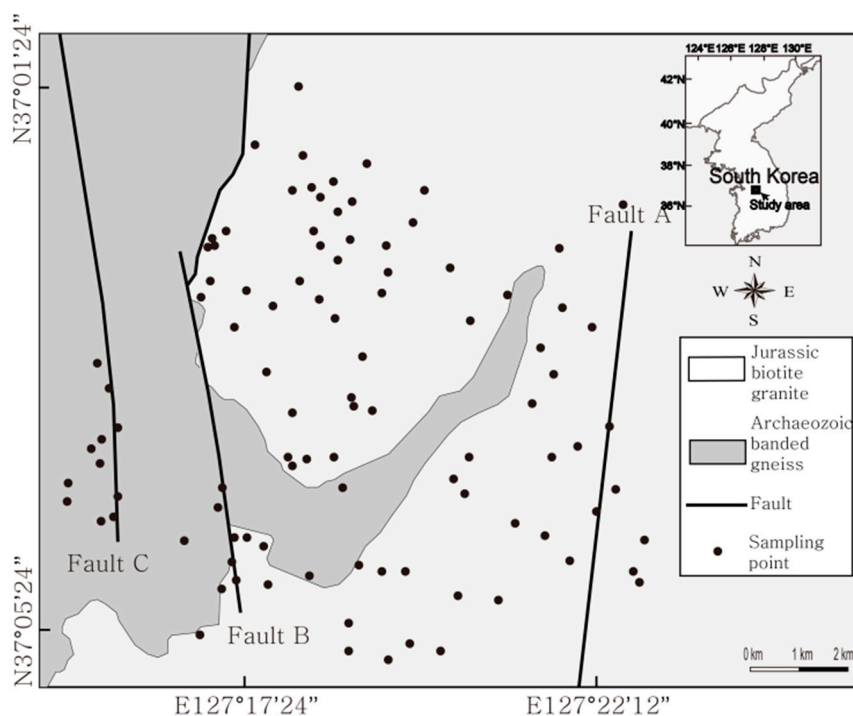


Figure 1. A simplified geological map of the sampling points in Yongin area, Korea.

2.3. ^{222}Rn and U Measurements

Groundwater samples were collected promptly to avoid radon gas loss. A total of 8 mL of each sample were injected and mixed with 12 mL of a commercial liquid scintillator cocktail solution (Optiphase Hisafe3, PerkinElmer). ^{222}Rn concentration was measured after 4 h elapsed for radioactive equilibrium between ^{222}Rn and its daughters. The ^{222}Rn concentration was measured using a liquid scintillation counter (LSC, Perkin Elmer, Wallac 1220 Quantulus) equipped with a pulse-shape analyzer which can electronically separate alpha and beta nuclides into different spectra. This ultra-low-level LSC is able to effectively measure very low-level alpha and beta nuclides, making it possible to optimize measurement conditions for various environmental radioactivity applications. The optimal pulse shape analysis (PSA) level was set to 100, determined using ^{241}Am and $^{90}\text{Sr}/^{90}\text{Y}$ standard radioactive solutions to minimize alpha/beta discrimination capabilities [26].

The detection efficiency for ^{222}Rn was determined based on the total peak area of the alpha line at 100 PSA level using the ^{226}Ra standard solution. Detection efficiency was determined in triplicate using three standard samples, demonstrating a mean value of 89% with standard deviation of 0.6%. Background values were measured in the 550–750 channel range, excluding the ^{214}Po peak region because ^{214}Po was immediately formed due to its short half-life.

Previously boiled ultra-pure water was mixed with a scintillation cocktail solution cleaned by argon gas to produce a background sample containing no radon. The background sample was measured for 5 h under the same protocol as actual samples. This background counting value was used to determine both the counting efficiency and detection limit. Based on Equation (1) [27], the minimum detectable activity (MDA, Bq L^{-1}) was calculated to be 0.22 Bq L^{-1} for the α -ray total peak.

$$\text{MDA} = \left(4.65 \times \sqrt{\frac{C_b}{t}} \right) / (E \times V \times 60), \quad (1)$$

where C_b (cpm) is the background count rate. V (L) and t (min) represent the sample volume (8 mL) and the background counting time, respectively. The ^{222}Rn concentration of the sample was determined using the following equation [28]:

$$C = (R_S - R_B) / (E \times V \times 60 \times (1 - \exp^{-\lambda t})), \quad (2)$$

where C (Bq L^{-1}) is the ^{222}Rn concentration of the sample. R_S (cpm) and R_B (cpm) represent the sample count rate and the background count rate, respectively. E is the counting efficiency. λ (day^{-1}) is the ^{222}Rn decay constant and t (day) is the elapsed time from sampling to the midpoint of the decay correction count.

Groundwater sample for the total U analysis was immediately filtered through $0.45 \mu\text{m}$ cellulose membrane, and then acidified to $\sim\text{pH } 2$ with nitric acid and stored in the vials which were pre-cleaned with nitric acid and de-ionized water. The concentration of U was measured using inductively coupled plasma mass spectrometry (ICP-MS; DRC-II; PerkinElmer). Calibrations were performed using U standard solution ($10 \mu\text{g mL}^{-1}$, Accustandard). The statistical and spatial analyses were performed using SPSS (SPSS Inc., v. 17, IBM, Armonk, NY, USA) and Grapher (Golden Software Inc., v. 13, Golden, CO, USA) respectively.

3. Results and Discussion

Well depth information, field parameters (temperature, EC, pH, and DO), and ^{222}Rn and U groundwater concentrations are shown in Table A1. We scrutinized the variables used in this study to examine unusual values. Groundwater was sampled from the wells of various depths, showing a temperature range of $11.9\text{--}18.5 \text{ }^\circ\text{C}$ (mean \pm standard deviation; $15.2 \pm 1.3 \text{ }^\circ\text{C}$). The EC, pH, and DO ranged from 68 to $712 \mu\text{S cm}^{-1}$ ($192 \pm 108 \mu\text{S cm}^{-1}$), from 5.1 to 8.9 (6.3 ± 0.6), and from 0.6 to 10.6 mg L^{-1} ($5.1 \pm 2.1 \text{ mg L}^{-1}$), respectively. The ^{222}Rn concentration in groundwater fell between 0.6 ± 0.1 and $673.7 \pm 8.7 \text{ Bq L}^{-1}$ with a mean value of $208 \pm 166 \text{ Bq L}^{-1}$. The U concentration in groundwater ranged from 0.02 to $117.00 \mu\text{g L}^{-1}$ with a mean value of $11.5 \pm 21.1 \mu\text{g L}^{-1}$. The highest concentrations of ^{222}Rn and U were observed at YI21 and YI32, respectively.

Histograms showing the frequency distributions of ^{222}Rn and U concentrations indicated that the concentrations of these radionuclides were skewed to the left (Figure 2). Approximately 50% of the sampling points showed ^{222}Rn concentrations below 148 Bq L^{-1} , and the distribution of U concentration showed approximately 10% of the sampling points were above $30 \mu\text{g L}^{-1}$.

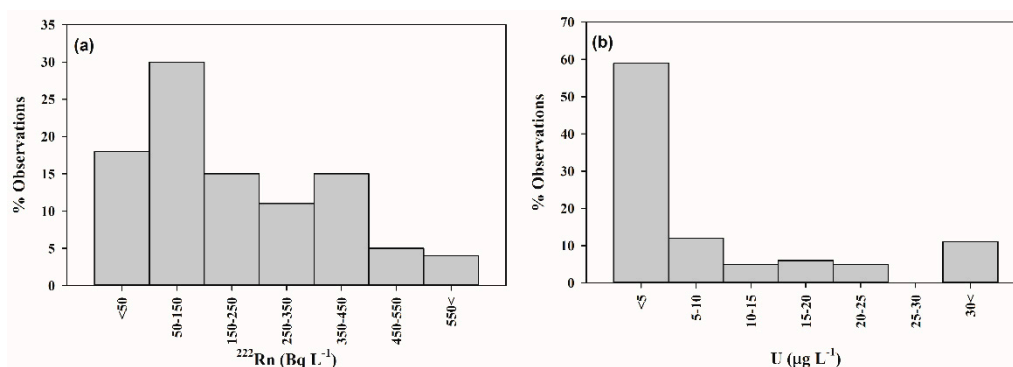


Figure 2. Histograms showing concentration frequency distributions for (a) radon (^{222}Rn) and (b) uranium (U) in the groundwater samples.

3.1. Correlations between ^{222}Rn or U and Field Parameters

The ^{222}Rn concentrations showed no significant correlation with temperature ($r = 0.04$, $p = 0.69$), EC ($r = 0.19$, $p = 0.06$), or DO ($r = 0.05$, $p = 0.63$) and only weak correlations with pH ($r = -0.29$, $p < 0.05$) (Figure 3). The U concentrations also showed no significant correlation with temperature ($r = 0.05$,

$p = 0.65$) or DO ($r = 0.16, p = 0.12$), and weak correlations with pH ($r = 0.30, p < 0.05$) and EC ($r = 0.27, p < 0.05$) (Figure 4). Even though the ^{222}Rn and U concentrations appeared to correspond with pH based on the statistical analysis, those data were highly scattered, and the correlation coefficients were extremely weak. Similar to the current results, prior research has reported neither significant nor weak correlation between pH and ^{222}Rn concentrations in groundwater [4,29]. These results therefore suggest that these individual field parameters may not play primary roles in regulating ^{222}Rn and U groundwater levels.

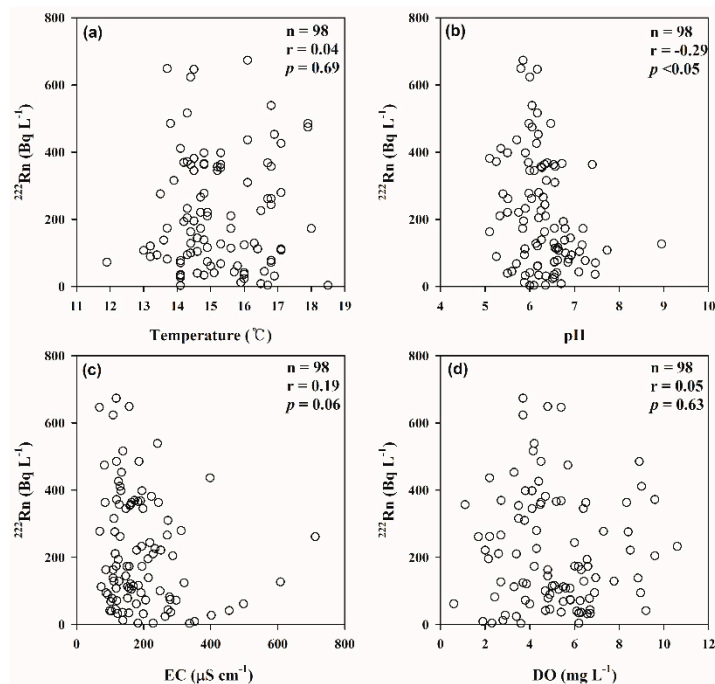


Figure 3. Scatter plots between ^{222}Rn and field parameters ((a) temperature; (b) pH; (c) EC; and (d) DO) in the groundwater samples.

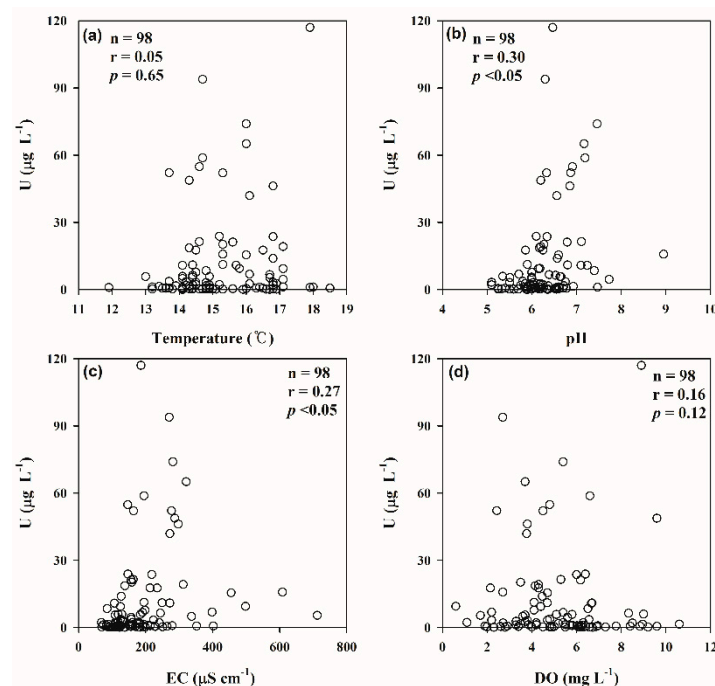


Figure 4. Scatter plots between U and field parameters ((a) temperature; (b) pH; (c) EC; and (d) DO) in the groundwater samples.

3.2. Effect of Lithology and Fault

For statistical analysis, the ^{222}Rn and U concentrations in groundwater were grouped based on the geological characteristics (granite or gneiss areas) of the sampling locations. The mean ^{222}Rn groundwater concentration in granite areas was $238 \pm 161 \text{ Bq L}^{-1}$, approximately four times higher than that of gneiss areas ($66 \pm 104 \text{ Bq L}^{-1}$), and the mean U groundwater concentration in granite areas ($14 \pm 23 \mu\text{g L}^{-1}$) was seven times higher than that in gneiss areas ($2 \pm 5 \mu\text{g L}^{-1}$). These results are similar to the previous studies conducted in various bedrock-type areas [2,30], reflecting the fact that granite contains high levels of radionuclides such as ^{226}Ra (parent of ^{222}Rn) and ^{238}U [31].

3.3. Spatial Distributions of ^{222}Rn and U

The spatial distributions of the ^{222}Rn and U groundwater concentrations also demonstrated relatively higher concentrations in granite than gneiss areas (Figure 5). To determine the spatial distribution, wells deeper than 30 m were selected to reduce data noise, specifically interactions between surface water and groundwater. Based on these spatial distributions, the highest concentrations (more than 600 Bq L^{-1}) of ^{222}Rn were observed near Fault A over granite bedrock (Figure 5a). This may be due to the fact that fractures with higher permeability/porosity can increase bedrock surface area in fault zones, allowing ^{222}Rn to dissolve from the bedrock into groundwater through active water-rock interactions. Previous studies have reported that fractures can enhance emanation surfaces, allowing ^{222}Rn to escape from rocks via α -recoil [32,33]. The relatively lower ^{222}Rn concentration in groundwater close to Faults B and C may be due to the different lithology (gneiss) of those well locations. The U concentrations displayed different distribution trends with higher U concentrations observed in the southern part of the studied area (Figure 5b). These different spatial distributions may be attributed to the fact that ^{222}Rn and U have different geochemical behavior: while the behavior of gaseous ^{222}Rn is determined by physical processes (e.g., groundwater movement) rather than chemical processes on the basis of the relationships between major ions (Na^+ , Mg^{2+} , and Cl^-) and ^{222}Rn concentrations [34,35], U concentrations in groundwater are controlled by redox potential and CO_2 partial pressure [24,36]. Similarly, several researches conducted in Korea have reported poor or weak relationships between ^{222}Rn and U concentrations [25,37,38]. Conversely, Singh et al. reported strong correlation ($r = 0.75$) between ^{222}Rn and ^{238}U concentrations in drinking water [3]. As such, more comprehensive and comparative investigation is required to better understand the behaviors of ^{222}Rn and U in groundwater with consideration to various chemical and physical processes including water mixing processes (groundwater-groundwater or groundwater-surface water).

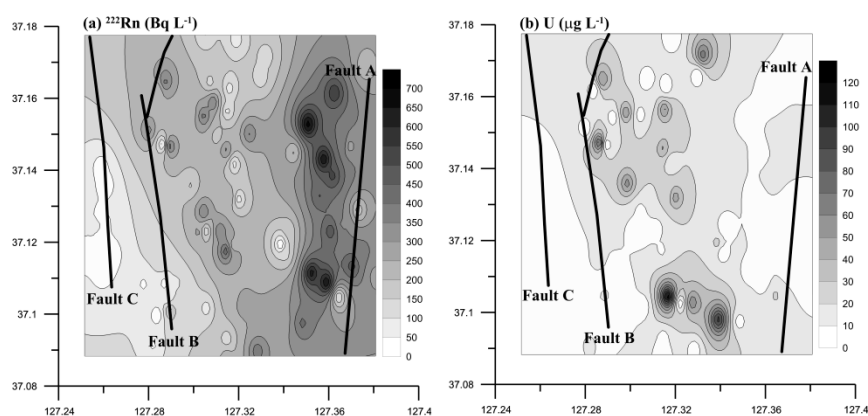


Figure 5. Spatial distributions of (a) ^{222}Rn (Bq L^{-1}) and (b) U ($\mu\text{g L}^{-1}$) in the groundwater samples (well depth > 30 m) with the different concentration scales ($0\text{--}700 \text{ Bq L}^{-1}$ for ^{222}Rn and $0\text{--}120 \mu\text{g L}^{-1}$ for U).

3.4. Effect of the Well Depth

The well depth of the 98 groundwater samples showed no significant statistical correlation with ^{222}Rn ($r = 0.10$, $p = 0.32$) or U ($r = 0.27$, $p = 0.15$) concentrations. For further granularity, wells located in granite area were classified as shallow (<30 m) or deep (>100 m) to investigate the effect of well depth on radionuclide concentration. While a significant positive correlation ($r = 0.68$, $p < 0.05$) was observed between ^{222}Rn and U concentrations in shallow wells, no significant relationship ($r = 0.27$, $p = 0.25$) was seen in deep groundwater wells (Figure 6). This result may be due to active groundwater-surface water interaction in shallow wells. In Korea, the mean depth of alluvial and/or weathering zone is generally less than 30 m. This zone tends to have higher hydraulic conductivity and be more fractured than bedrock. Since more active groundwater-surface water interaction can be occurred in the shallow wells, and surface water has lower ^{222}Rn and U concentrations than groundwater [25], the concentrations of these radionuclides in the shallow wells were relatively lower than those of the deep wells and showed a significant positive correlation depending on the surface water mixing rate. The poor correlation of concentrations in the deep wells may be due to different behaviors of ^{222}Rn and U in groundwater (described in detail above).

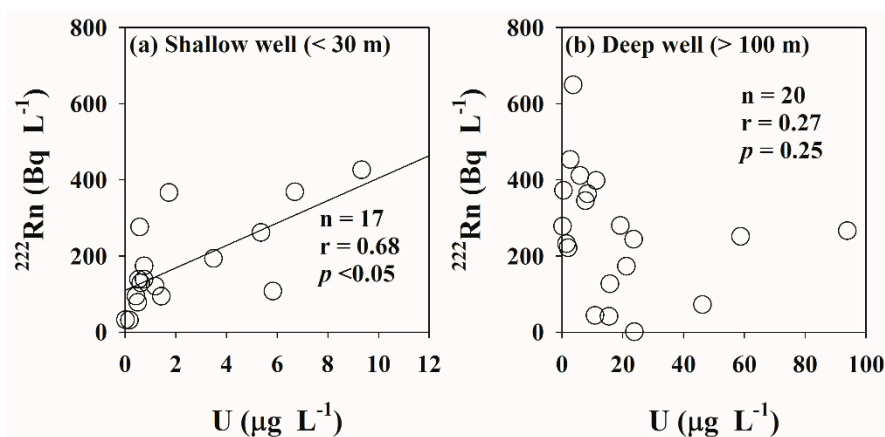


Figure 6. Scatter plots showing ^{222}Rn and U in the groundwater samples from the shallow (a) and deep (b) wells in the granite area. Note different scale of the axes.

3.5. Temporal Variation in ^{222}Rn

To determine a temporal variation of ^{222}Rn concentrations in shallow wells (<30 m) with relatively active groundwater-surface water interaction, groundwater sampling campaigns were conducted in five wells throughout August, October, and November, 2013. The temporal variations of ^{222}Rn concentration in these well showed similar trends, except for YI100. ^{222}Rn concentrations of the other four wells in October were about two times higher than that in August. This result may reflect the higher precipitation rate in July (Figure 7), because ^{222}Rn concentration in groundwater should be decreased by an inflow of rainwater or surface water into shallow groundwater following large rainfall events in the summer monsoon season (June and July). In November, the ^{222}Rn concentrations decreased, potentially related to the regional groundwater use. Although information on seasonal groundwater use was not obtained in this study, water curtain cultivation has been conducted using groundwater in winter season to maintain high air temperature in vinyl houses in this study area. This continuous groundwater extraction increases groundwater circulation, decreasing the groundwater radon concentration [5] due to an input of water from rivers or streams, which have low ^{222}Rn concentrations. Therefore, these results suggest continuous monitoring or a minimum of bi-weekly measurements of naturally occurring radionuclides in groundwater are required not only to reduce health risks but also to better understand groundwater-surface water interactions.

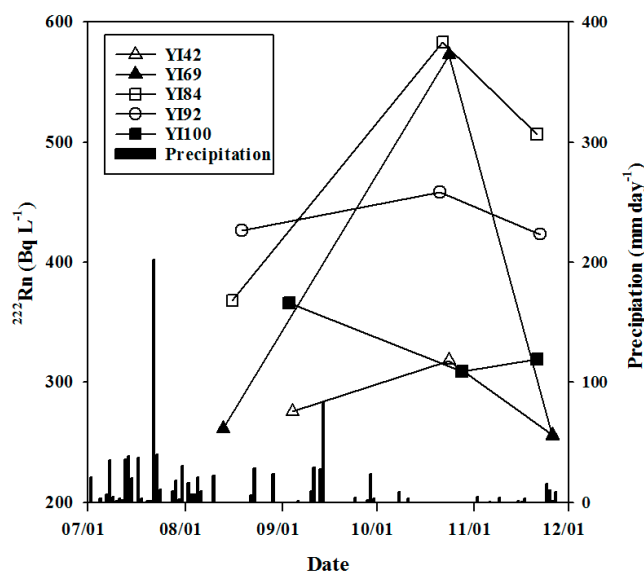


Figure 7. Temporal variations in ^{222}Rn concentrations in the shallow (<30 m) groundwater wells in August, October, and November 2013.

4. Conclusions

^{222}Rn and U concentrations were measured in 98 groundwater wells in Yongin area, Korea. Results revealed that the ^{222}Rn concentrations of approximately 50% of the sampling points in the study area was higher than 148 Bq L^{-1} (the AMCL recommended by the US EPA), and 10% of the sampling points displayed U concentrations above $30 \mu\text{g L}^{-1}$ (the WHO guideline level for drinking water). Based on statistical analyses, geological variability, well depth, rainfall rates, and geological structures (faults) may affect the levels, temporal variations, and spatial distributions of ^{222}Rn and U in groundwater. Our results suggest that continuous or short interval monitoring of ^{222}Rn and U in groundwater, especially that used for drinking, is required to reduce potential health risks via the intake of groundwater containing high levels of these naturally occurring radionuclides.

Author Contributions: B.W.C. and S.Y.C. conceived the study and conducted the sampling and analysis for the study. S.Y.C., M.-H.K., B.W.C., Y.-Y.J., and Y.H.O. interpreted the data and contributed to the discussion. Y.H.O. and Y.-Y.J. created the figures and tables. The manuscript was written in a joint effort between S.Y.C. and Y.H.O.

Funding: This research was supported by the Basic Research Project (GP2017-008) of the Korea Institute of Geoscience and Mineral Resources (KIGAM), funded by the Ministry of Science, ICT and Future, and National Institute of Environmental Research (NIER-SP2015-386).

Conflicts of Interest: The authors declare no conflict of interest.

Appendix A

Table A1. Well depth, field parameters including temperature, electrical conductivity (EC), pH, and dissolved oxygen (DO), and the concentrations of ^{222}Rn and U in groundwater of Yongin area in 2013.

Sampling Point No.	Well Depth (m)	Temp. ($^{\circ}\text{C}$)	EC ($\mu\text{S cm}^{-1}$)	pH	DO (mg L^{-1})	^{222}Rn (Bq L^{-1})	U ($\mu\text{g L}^{-1}$)
YI01	78	14.1	402	6.5	2.9	27.4 ± 1.1	0.66 ± 0.01
YI02	200	15.3	608	8.9	2.7	126.7 ± 2.6	15.80 ± 0.27
YI03	30	15.3	102	5.7	5.5	68.1 ± 1.8	0.20 ± 0.01
YI04	200	16.0	455	6.6	4.7	41.5 ± 1.4	15.50 ± 0.27
YI05	40	17.1	152	6.6	5.5	112.2 ± 2.5	1.20 ± 0.01
YI06	45	16.6	116	5.6	4.9	45.2 ± 1.4	0.15 ± 0.01

Table A1. Cont.

Sampling Point No.	Well Depth (m)	Temp. (°C)	EC ($\mu\text{S cm}^{-1}$)	pH	DO (mg L^{-1})	^{222}Rn (Bq L^{-1})	U ($\mu\text{g L}^{-1}$)
YI07	80	18.5	228	6.0	6.2	3.7 ± 0.4	0.61 ± 0.01
YI08	80	16.5	352	6.7	1.9	8.5 ± 0.6	0.63 ± 0.01
YI09	100	14.9	279	6.5	5.8	74.1 ± 1.8	0.81 ± 0.01
YI10	200	14.7	270	6.3	2.7	265.9 ± 4.4	93.90 ± 1.60
YI11	25	13.0	118	6.6	5.8	107.4 ± 2.3	5.83 ± 0.05
YI12	120	16.0	264	6.5	3.4	23.7 ± 0.7	0.45 ± 0.01
YI13	150	15.9	138	5.8	2.8	12.2 ± 0.4	0.08 ± 0.01
YI14	120	15.8	498	6.8	0.6	61.5 ± 1.2	9.42 ± 0.07
YI15	100	15.0	178	6.1	4.0	60.7 ± 1.2	0.25 ± 0.01
YI16	100	13.9	111	6.3	3.5	315.6 ± 4.4	1.67 ± 0.02
YI17	90	15.3	164	6.3	4.5	363.3 ± 4.9	52.10 ± 0.89
YI18	80	15.6	115	5.3	2.6	210.7 ± 3.1	0.42 ± 0.01
YI19	80	14.9	228	6.3	3.4	210.0 ± 3.1	0.43 ± 0.01
YI20	100	16.8	241	6.0	4.2	538.9 ± 7.1	2.08 ± 0.02
YI21	100	16.1	118	5.8	3.7	673.7 ± 8.7	2.61 ± 0.02
YI22	100	14.5	68	6.1	5.4	646.7 ± 8.4	2.21 ± 0.02
YI23	120	17.1	312	6.2	4.3	279.6 ± 3.9	19.20 ± 0.33
YI24	100	14.3	138	6.1	4.15	516.7 ± 6.8	18.60 ± 0.32
YI25	150	16.9	134	6.1	3.3	453.0 ± 6	2.71 ± 0.02
YI26	100	18.0	150	5.8	4.2	173.0 ± 2.6	1.17 ± 0.01
YI27	50	14.4	87	6.3	4.8	163.0 ± 2.5	0.27 ± 0.01
YI28	100	13.8	119	5.9	4.5	485.6 ± 6.4	0.23 ± 0.01
YI30	120	14.7	195	7.2	6.6	251.5 ± 3.8	58.80 ± 1.00
YI31	100	14.4	109	5.1	6.3	286.3 ± 4.2	2.11 ± 0.02
YI32	100	17.9	186	6.4	8.9	239.3 ± 3.7	117.00 ± 1.99
YI33	120	14.1	129	5.3	9.0	411.1 ± 5.7	5.93 ± 0.05
YI34	120	14.9	179	5.7	8.5	221.1 ± 3.4	2.00 ± 0.02
YI35	100	14.5	223	5.1	4.7	381.5 ± 5.4	3.23 ± 0.03
YI36	70	14.1	337	6.0	3.6	3.0 ± 0.3	4.95 ± 0.04
YI37	100	14.6	104	5.5	6.1	39.6 ± 1.0	0.25 ± 0.01
YI38	100	13.2	93	5.2	4.9	89.3 ± 1.7	0.20 ± 0.01
YI39	50	14.7	251	5.5	2.0	221.1 ± 3.4	0.30 ± 0.01
YI40	200	15.7	272	7.1	6.7	43.7 ± 1.1	10.9 ± 0.19
YI41	100	14.3	287	6.2	9.6	204.4 ± 3.1	48.80 ± 0.83
YI42	25	13.5	114	5.4	8.4	275.9 ± 4.0	0.58 ± 0.01
YI43	120	14.3	194	5.9	10.6	232.2 ± 3.5	1.46 ± 0.02
YI44	120	14.3	119	5.2	9.6	371.9 ± 5.2	0.48 ± 0.01
YI45	100	14.8	156	6.2	6.2	34.1 ± 0.9	0.38 ± 0.01
YI46	150	14.1	137	6.5	6.3	35.9 ± 0.9	0.15 ± 0.01
YI47	100	15.1	99	6.0	9.2	41.1 ± 1.0	0.15 ± 0.01
YI48	100	16.7	183	6.3	2.3	4.1 ± 0.3	0.08 ± 0.01
YI49	130	14.8	85	7.4	6.5	363.3 ± 5.1	8.42 ± 0.06
YI50	100	14.6	163	7.1	5.3	104.4 ± 1.9	21.40 ± 0.37
YI51	30	13.2	161	6.1	3.8	120.7 ± 2.6	1.19 ± 0.01
YI52	30	14.1	122	5.9	6.7	32.6 ± 1.2	0.02 ± 0.01
YI53	35	11.9	206	6.5	5.8	72.6 ± 1.9	0.92 ± 0.01
YI54	30	13.4	88	6.9	8.9	94.1 ± 2.2	1.43 ± 0.02
YI55	30	13.6	109	6.7	8.8	138.1 ± 2.9	0.53 ± 0.01
YI56	35	16.3	111	6.5	7.7	128.9 ± 2.8	0.62 ± 0.01
YI57	30	16.9	199	6.3	6.5	31.5 ± 1.1	0.17 ± 0.01
YI58	100	13.7	277	6.8	2.4	81.9 ± 2.0	52.20 ± 0.89
YI59	33	14.8	214	6.2	6.9	138.9 ± 2.8	0.75 ± 0.01
YI60	150	15.6	157	6.7	6.1	173.0 ± 3.3	21.20 ± 0.37
YI61	30	16.1	272	6.5	3.7	310.0 ± 5.0	41.90 ± 0.72
YI62	50	14.1	107	7.2	6.6	77.4 ± 2.0	10.80 ± 0.19

Table A1. Cont.

Sampling Point No.	Well Depth (m)	Temp. (°C)	EC ($\mu\text{S cm}^{-1}$)	pH	DO (mg L^{-1})	^{222}Rn (Bq L^{-1})	U ($\mu\text{g L}^{-1}$)
YI63	30	14.2	173	5.9	2.7	369.3 \pm 5.7	2.01 \pm 0.02
YI64	50	16.8	127	6.5	4.4	357.4 \pm 5.5	13.90 \pm 0.24
YI65	37	14.4	126	6.1	6.4	128.5 \pm 2.6	0.55 \pm 0.01
YI66	30	14.3	192	5.8	6.9	94.4 \pm 2.1	0.43 \pm 0.01
YI67	100	14.4	249	6.8	4.6	99.6 \pm 2.2	11.00 \pm 0.19
YI68	100	14.4	244	6.5	8.3	363.3 \pm 5.7	6.38 \pm 0.05
YI69	30	16.7	712	5.5	1.7	261.5 \pm 3.8	5.36 \pm 0.04
YI70	100	15.2	161	6.2	1.1	357.0 \pm 5.0	2.26 \pm 0.02
YI71	90	16.4	730	5.8	3.3	112.2 \pm 2.0	1.13 \pm 0.01
YI72	90	16.5	234	6.2	4.3	225.9 \pm 3.4	17.60 \pm 0.30
YI73	50	16.1	398	5.7	2.2	436.7 \pm 6.1	6.87 \pm 0.05
YI74	100	16.8	130	6.0	2.2	261.9 \pm 4.0	3.20 \pm 0.03
YI75	100	14.6	146	6.9	4.8	144.4 \pm 2.5	54.90 \pm 0.94
YI76	100	16.0	281	7.4	5.4	36.3 \pm 0.9	74.00 \pm 1.26
YI77	100	15.6	169	6.5	5.0	114.4 \pm 1.9	0.36 \pm 0.01
YI78	100	15.3	159	6.2	3.5	354.1 \pm 4.9	20.20 \pm 0.35
YI79	100	14.5	213	5.8	2.1	195.2 \pm 2.9	17.60 \pm 0.30
YI80	150	15.3	195	5.9	4.1	398.1 \pm 5.3	11.20 \pm 0.20
YI81	170	14.5	198	6.0	4.1	345.2 \pm 4.7	7.71 \pm 0.06
YI82	80	14.8	132	5.5	3.8	132.2 \pm 2.1	3.15 \pm 0.03
YI83	150	15.2	147	6.1	6.4	0.6 \pm 0.1	23.80 \pm 0.41
YI84	25	16.7	191	6.3	5.4	368.1 \pm 4.9	6.70 \pm 0.05
YI85	100	17.9	83	6.0	5.7	474.4 \pm 6.2	0.94 \pm 0.01
YI86	200	14.8	69	5.9	7.3	277.8 \pm 3.9	0.23 \pm 0.01
YI87	170	13.7	157	5.8	4.8	648.9 \pm 8.3	3.69 \pm 0.03
YI88	100	14.4	109	6.0	3.7	623.7 \pm 8.0	5.53 \pm 0.04
YI89	200	16.8	297	6.8	3.8	72.2 \pm 1.4	46.20 \pm 0.79
YI90	200	16.8	218	6.3	6.0	243.7 \pm 3.5	23.60 \pm 0.41
YI91	50	14.9	184	6.6	5.1	116.3 \pm 1.9	5.80 \pm 0.05
YI92	25	17.1	125	6.1	4.4	426.3 \pm 5.7	9.34 \pm 0.07
YI93	100	17.1	157	7.7	5.6	108.1 \pm 1.8	4.53 \pm 0.04
YI94	50	14.1	120	7.4	6.2	70.7 \pm 1.5	1.06 \pm 0.01
YI96	30	13.7	118	6.5	6.0	173.7 \pm 2.8	0.75 \pm 0.01
YI97	30	14.2	124	6.7	6.5	193.3 \pm 3.0	3.49 \pm 0.03
YI98	50	16.0	321	7.1	3.7	124.1 \pm 2.2	65.10 \pm 1.11
sYI99	30	16.8	152	6.6	4.8	78.1 \pm 1.6	0.50 \pm 0.01
YI100	30	14.8	183	6.7	5.1	366.3 \pm 5.2	1.73 \pm 0.02

References

- Morris, B.L.; Lawrence, A.R.L.; Chilton, P.J.C.; Adams, B.; Calow, R.C.; Klinck, B.A. Groundwater and its Susceptibility to Degradation: A Global Assessment of the Problem and Options for Management. In *Early Warning and Assessment Report Series RS 03-3*; United Nations Environment Programme (UNEP): Nairobi, Kenya, 2003.
- Lee, J.Y. Environmental issues of groundwater in Korea: Implications for sustainable use. *Environ. Conserv.* **2011**, *38*, 64–74. [[CrossRef](#)]
- Singh, P.; Singh, P.; Sahoo, B.K.; Bajwa, B.S. A study on uranium and radon levels in drinking water sources of a mineralized zone of Himachal Pradesh, India. *J. Radioanal. Nucl. Chem.* **2016**, *309*, 541–549. [[CrossRef](#)]
- Thivya, C.; Chidambaram, S.; Thilagavathi, R.; Tirumalesh, K.; Nepolian, M.; Prasanna, M.V. Spatial and temporal variations of radon concentrations in groundwater of hard rock aquifers in Madurai district, India. *J. Radioanal. Nucl. Chem.* **2017**, *313*, 603–609. [[CrossRef](#)]
- Asare-Donkor, N.K.; Poku, P.A.; Addison, E.C.D.K.; Wemengah, D.D.; Adimado, A.A. Measurement of radon concentration in groundwater in the Ashanti region of Ghana. *J. Radioanal. Nucl. Chem.* **2018**, *317*, 675–683. [[CrossRef](#)]

6. Avery, E.; Bibby, R.; Visser, A.; Esser, B.; Moran, J. Quantification of Groundwater Discharge in a Subalpine Stream Using Radon-222. *Water* **2018**, *10*, 100. [[CrossRef](#)]
7. Schubert, M.; Knöller, K.; Stollberg, R.; Mallast, U.; Ruzsa, G.; Melikadze, G. Evidence for Submarine Groundwater Discharge into the Black Sea—Investigation of Two Dissimilar Geographical Settings. *Water* **2017**, *9*, 468. [[CrossRef](#)]
8. Schubert, M.; Knoeller, K.; Rocha, C.; Einsiedl, F. Evaluation and source attribution of freshwater contributions to Kinvarra Bay, Ireland, using ^{222}Rn , EC and stable isotopes as natural indicators. *Environ. Monit. Assess.* **2015**, *187*, 105. [[CrossRef](#)]
9. Cartwright, I.; Hofmann, H.; Sirianos, M.A.; Weaver, T.R.; Simmons, C.T. Geochemical and ^{222}Rn constraints on baseflow to the Murray River, Australia, and timescales for the decay of low-salinity groundwater lenses. *J. Hydrol.* **2011**, *405*, 333–343. [[CrossRef](#)]
10. Cook, P.G.; Wood, C.; White, T.; Simmons, C.T.; Fass, T.; Brunner, P. Groundwater inflow to a shallow, poorly-mixed wetland estimated from a mass balance of radon. *J. Hydrol.* **2008**, *354*, 213–226. [[CrossRef](#)]
11. Barberio, M.; Gori, F.; Barbieri, M.; Billi, A.; Devoti, R.; Doglioni, C.; Petitta, M.; Riguzzi, F.; Rusi, S. Diurnal and Semidiurnal Cyclicity of Radon (^{222}Rn) in Groundwater, Giardino Spring, Central Apennines, Italy. *Water* **2018**, *10*, 1276. [[CrossRef](#)]
12. Kuo, T. Correlating precursory declines in groundwater radon with earthquake magnitude. *Groundwater* **2014**, *52*, 217–224. [[CrossRef](#)] [[PubMed](#)]
13. Igarashi, G.; Saeki, S.; Takahata, N.; Sumikawa, K.; Tasaka, S.; Sasaki, Y.; Takahashi, M.; Sano, Y. Groundwater radon anomaly before the Kobe Earthquake in Japan. *Science* **1995**, *269*, 60–61. [[CrossRef](#)] [[PubMed](#)]
14. Rodrigo, J.F.; Casas-Ruiz, M.; Vidal, J.; Barbero, L.; Baskaran, M.; Ketterer, M.E. Application of $^{234}\text{U}/^{238}\text{U}$ activity ratios to investigations of subterranean groundwater discharge in the Cadiz coastal area (SW Spain). *J. Environ. Radioact.* **2014**, *130*, 68–71. [[CrossRef](#)] [[PubMed](#)]
15. Wang, R.-M.; You, C.-F. Uranium and strontium isotopic evidence for strong submarine groundwater discharge in an estuary of a mountainous island: A case study in the Gaoping River Estuary, Southwestern Taiwan. *Mar. Chem.* **2013**, *157*, 106–116. [[CrossRef](#)]
16. Todorovic, N.; Nikolov, J.; Forkapic, S.; Bikit, I.; Mrdja, D.; Krmar, M.; Veskovc, M. Public exposure to radon in drinking water in Serbia. *Appl. Radiat. Isot.* **2012**, *70*, 543–549. [[CrossRef](#)]
17. Ravikumar, P.; Somashekar, R. Determination of the radiation dose due to radon ingestion and inhalation. *Int. J. Environ. Sci. Technol.* **2014**, *11*, 493–508. [[CrossRef](#)]
18. Kurttio, P.; Komulainen, H.; Leino, A.; Salonen, L.; Auvinen, A.; Saha, H. Bone as a possible target of chemical toxicity of natural uranium in drinking water. *Environ. Health Perspect.* **2004**, *113*, 68–72. [[CrossRef](#)]
19. Zamora, M.L.; Tracy, B.; Zielinski, J.; Meyerhof, D.; Moss, M. Chronic ingestion of uranium in drinking water: A study of kidney bioeffects in humans. *Toxicol. Sci.* **1998**, *43*, 68–77. [[CrossRef](#)]
20. Ayotte, J.D.; Gronberg, J.M.; Apodaca, L.E. Trace elements and radon in groundwater across the United States, 1992–2003. In *Scientific Investigation Report 2011–5059*; U.S. Geological Survey: Reston, VA, USA, 2011.
21. Cho, B.W.; Kim, H.K.; Kim, M.S.; Hwang, J.H.; Yoon, U.; Cho, S.Y.; Choo, C.O. Radon concentrations in the community groundwater system of South Korea. *Environ. Monit. Assess.* **2019**, *191*, 189. [[CrossRef](#)]
22. WHO. *Guidelines for Drinking-Water Quality*, 4th ed.; WHO: Geneva, Switzerland, 2011.
23. Shin, W.; Oh, J.; Choung, S.; Cho, B.W.; Lee, K.S.; Yun, U.; Woo, N.C.; Kim, H.K. Distribution and potential health risk of groundwater uranium in Korea. *Chemosphere* **2016**, *163*, 108–115. [[CrossRef](#)]
24. Hwang, J.; Kim, T.; Kim, H.; Cho, B.; Lee, S. Predictive radon potential mapping in groundwater: A case study in Yongin, Korea. *Environ. Earth Sci.* **2017**, *76*, 515–527. [[CrossRef](#)]
25. Jeong, C.H.; Yang, J.H.; Lee, Y.C.; Lee, Y.J.; Cho, H.Y.; Kim, M.S.; Kim, H.K.; Kim, T.S.; Jo, B.U. Occurrence characteristics of uranium and radon-222 in groundwater at ○○ Village, Yongin area. *J. Eng. Geol.* **2016**, *26*, 261–276. [[CrossRef](#)]
26. Kim, Y.; Cho, S.-Y.; Yoon, Y.-Y.; Lee, K.-Y. Optimal method of radon analysis in groundwater using ultra low-level liquid scintillation counter. *J. Soil Groundw. Environ.* **2006**, *11*, 59–66, (In Korean with English abstract).
27. Currie, L.A. Limits for qualitative detection and quantitative determination, application to radiochemistry. *Anal. Chem.* **1968**, *40*, 589–593. [[CrossRef](#)]
28. Hohorst, F.A.; Huntley, M.W.; Hantenstein, S.D. *Determination of Radium in Water*; Idaho National Engineering Laboratory: Idaho Falls, ID, USA, 1995.

29. Bartlett, T.R.; Morrison, S.J. Tracer method to determine residence time in a permeable reactive barrier. *Groundwater* **2009**, *47*, 598–604. [[CrossRef](#)] [[PubMed](#)]
30. Krachler, R.; Krachler, R.; Gulce, F.; Keppler, B.K.; Wallner, G. Uranium concentrations in sediment pore waters of Lake Neusiedl, Austria. *Sci. Total Environ.* **2018**, *633*, 981–988. [[CrossRef](#)] [[PubMed](#)]
31. Asumadu-Sakyi, A.B.; Oppon, O.C.; Quashie, F.K.; Adjei, C.A.; Akortia, E.; Nsiah-Akoto, I.; Appiah, K. Levels and potential effect of radon gas in groundwater of some communities in the Kassena Nankana district of the Upper East region of Ghana. *Proc. Int. Acad. Ecol. Environ. Sci.* **2012**, *2*, 223–233.
32. Khattak, N.U.; Khan, M.A.; Shah, M.T.; Ali, N. Radon concentration in drinking water sources of the region adjacent to a tectonically active Karak Thrust, southern Kohat Plateau, Khyber Pakhtunkhwa, Pakistan. *J. Radioanal. Nucl. Chem.* **2014**, *302*, 315–329. [[CrossRef](#)]
33. Erdogan, M.; Eren, N.; Demirel, S.; Zedef, V. Determination of radon concentration levels in well water in Konya, Turkey. *Radiat. Prot. Dosim.* **2013**, *156*, 489–494. [[CrossRef](#)]
34. Telahigue, F.; Agoubi, B.; Souid, F.; Kharroubi, A. Groundwater chemistry and radon-222 distribution in Jerba Island, Tunisia. *J. Environ. Radioact.* **2018**, *182*, 74–84. [[CrossRef](#)]
35. Roba, C.A.; Codrea, V.; Moldovan, M.; Baciu, C.; Cosma, C. Radon and radium content of some cold and thermal aquifers from Bihor County (northwestern Romania). *Geofluids* **2010**, *10*, 571–585. [[CrossRef](#)]
36. Murphy, W.M.; Shock, E.L. Environmental aqueous geochemistry of actinides. *Rev. Mineral. Geochem.* **1999**, *38*, 221–253.
37. Jeong, C.H.; Yang, J.H.; Lee, Y.J.; Lee, Y.C.; Choi, H.Y.; Kim, M.S.; Kim, H.K.; Kim, T.S.; Jo, B.U. Occurrences of uranium and radon-222 from groundwaters in various geological environment in the Hoengseong area. *J. Eng. Geol.* **2015**, *25*, 557–576. [[CrossRef](#)]
38. Cho, B.W.; Kim, M.S.; Kim, T.S.; Han, J.S.; Yun, U.; Lee, B.D.; Hwang, J.H.; Choo, C.O. Hydrochemistry and distribution of uranium and radon in groundwater of the Nonsan area. *J. Eng. Geol.* **2012**, *22*, 427–437. [[CrossRef](#)]



© 2019 by the authors. Licensee MDPI, Basel, Switzerland. This article is an open access article distributed under the terms and conditions of the Creative Commons Attribution (CC BY) license (<http://creativecommons.org/licenses/by/4.0/>).